A Wavelength-Shifting Fluorescent Probe for Investigating Physical Aging

Otto van den Berg, Wolter F. Jager,* Daniele Cangialosi,‡ Jan van Turnhout, Peter J. T. Verheijen,† Michael Wübbenhorst,§ and Stephen J. Picken*

Faculty of Applied Sciences, Department of Polymer Materials and Engineering, Delft University of Technology, Julianalaan 136, 2628BL Delft, The Netherlands, and Dutch Polymer Institute, PO Box 902, 5600 AX Eindhoven, The Netherlands

Received August 13, 2004; Revised Manuscript Received October 3, 2005

ABSTRACT: 7-(Dimethylamino)-1-methylquinolinium tetrafluoroborate (**2**), a stable color shifting mobility sensitive fluorescent probe, was employed for investigating physical aging in amorphous polymers. A linear correlation between the emission wavelength of **2** and the specific volume of the polymer was found in polycarbonate (PC) and poly(methyl methacrylate) (PMMA). The shift in emission wavelength measured during physical aging was used to calculate the temperature and time dependence of the effective relaxation time τ_{eff}, employing an age-dependent Kohlrausch−Williams−Watts (KWW) equation. From these data and by comparison with data obtained by positron annihilation spectroscopy (PALS) in PC and volume relaxation in PC and PMMA, it was concluded that the fluorescence of **2** yields reliable information on physical aging of these polymers. The fluorescence method, employing a color-shifting probe, offers opportunities for investigating physical aging in powders and semicrystalline polymers, of specific components in blends and mixtures, and in confined systems.

Introduction

When amorphous polymers are cooled below the glass transition temperature, they fall out of equilibrium. The subsequent time evolution of properties like volume,[1,2] enthalpy,[3,4] and creep toward equilibrium is a self-retarding process that is known as physical aging. Many studies have been made on the impact of physical aging on the mechanical properties of amorphous polymers.[5] Excellent reviews on physical aging of polymers and glass-forming liquids have been published.[6−8] Since physical aging has a profound influence, in particular on the long-term properties of polymers, a better understanding of this phenomenon is of great practical importance.

In addition, physical aging provides information about the dynamics of supercooled liquids. Several reports on the behavior of both polymeric and nonpolymeric glass formers just below the glass transition temperature T_g have been published recently.[9−11] These studies showed that the non-Arrhenius temperature dependence of the relaxation time of the α-process, usually well described by the phenomenological Vogel−Fulcher−Tammann (VFT) equation,[12−14] is replaced by a weaker temperature dependence. In a narrow temperature range below T_g this dependence can be described by an Arrhenius law.[15]

Fluorescent probes that detect medium mobility by changes in the emission intensity are known for a considerable time. Malononitrile-based fluorescent dyes, so-called rotor probes,[16] dominate this field of research. The singlet excited state of the dye has two major pathways to return to the ground state. The first and most common pathway is radiationless decay, a process that involves rotation within the excited molecule and requires free volume. The second pathway involves the emission of a photon from the planar molecule, which is only probable when rotation within the excited state is sterically hindered. Physical aging lowers the amount of free volume available for probe rotation and thus leads to an increase in emission intensity. The response of "rotor probe" doped in various polymers[17] showed asymmetry behavior and memory effects,[18] similar to those published for specific volume recovery experiments.[19] Recently, physical aging in thin films was investigated using the same type of probe molecule.[20] Although mobility is probed on a molecular scale, a direct connection between the bulk volume response and the response of the ensemble of fluorescent probes has been established.[21]

Replacing intensity-changing fluorescent probes by wavelength-shifting ones would be a major improvement. Besides the intrinsic advantages of using fluorescent probes, such as the nondestructive nature of this technique that allows for remote sensing, fast acquisition that allows for on-line monitoring, and a relative freedom of sample size and geometry, wavelength-shifting probes offer additional advantages. Since the emission wavelength is a state variable, wavelength-shifting probes are self-referencing. This opens up a larger application window, since most requirements concerning sample composition and geometry, which limit the use of intensity changing probes, do not apply. Therefore, in addition to homogeneous, optically clear samples of well-controlled thickness, opaque and even light-scattering samples are accessible using wavelength-shifting probes.[22]

Wavelength-shifting mobility-sensitive fluorescent probes generally belong to two classes of materials: the charge transfer (CT) and the charge resonance (CR) probes. CT probes have either a D-π-A[23] or D-σ-A[24] architecture, and CR probes are organic salts of the D-π-A^+X^- type.[25] Both classes of probes have been used for monitoring polymerization processes[23−25] and for polymer characterization,[26−29] but not for measuring physical aging.

† Faculty of Applied Sciences, Department of Process Systems Engineering, Delft University of Technology.

‡ Present address: Fundacion Donostia International Physics Center, Paseo Manuel de Lardizabal 4, 20018 San Sebastián, Spain.

§ Present address: Laboratory for Acoustics and Thermal Physics, Department of Physics and Astronomy, Katholieke Universiteit Leuven, Celestijnenlaan 200 D, B-3001 Leuven, Belgium.

* Corresponding authors: W. F. Jager (W.F.Jager@tnw.tudelft.nl) or S. J. Picken (S.J.Picken@tnw.tudelft.nl).

10.1021/ma048329i CCC: $33.50
Published on Web 11/30/2005

In this paper we present 7-(dimethylamino)-1-methylquinolinium tetrafluoroborate (**2**), as the first mobility-sensitive fluorescent probe that monitors physical aging by shifting the color of its emission. We will demonstrate the ability of this probe to monitor physical aging in PC and PMMA in a broad range of temperatures. Results obtained by positron annihilation lifetime spectroscopy (PALS)[30] in PC and volume relaxation experiments in PC and PMMA were used as a reference, to check the reliability of the probe technique. The fluorescent probe method turns out to offer a versatile and reliable method to measure physical aging across a wide range of temperatures without undue limitations concerning sample size, geometry, or composition. We attribute the success of this methodology to the ability of the probe to detect changes in specific volume and its high thermal and photochemical stability.

Modeling of the Kinetics of Physical Aging Studied by Wavelength-Shifting Fluorescent Probes. During physical aging the emission of **2** shifts to the blue, and this blue shift originates from the decrease in mobility of the polar groups in the host polymer. The time dependence of the blue shift during aging at a constant temperature can be modeled in various ways. For early summaries of several functions to model physical aging, in particular of the decrease in specific volume, we refer to refs 1 and 31. Nowadays, the stretched exponential, or the Kohlrausch−Williams−Watts (KWW) function, is mostly used as a basis:[6−8]

$$\Phi(t) = \exp\left[-\left(\frac{t}{\tau}\right)^b\right] \qquad 1 \geq b > 0 \tag{1}$$

Here b is the KWW stretching parameter that determines the broadness of a distribution of relaxation times. The age-dependent KWW function (AD-KWW) can be derived by partitioning the relaxation time τ in a thermally activated part τ_T and an age-dependent part τ_a:

$$\tau(T,t) = \tau_T \tau_a(t) \tag{2}$$

The increase of the age dependent-part τ_a can be described by a power law,[32] in which t is scaled to t_s:[33]

$$\tau_a(t) = (1 + t/t_s)^a \qquad 1 \geq a > 0 \tag{3}$$

Here a is the aging power. Obviously, aging with the highest degree of self-retardation, so-called "logarithmic" aging, occurs if $a = 1$.

By inserting eqs 2 and 3 into the KWW equation (1), in which t/τ in the exponential has to be replaced by $\int_0^t dt'/\tau(T,t')$, the age-dependent KWW function for modeling physical aging with a wavelength shifting fluorescent probe is obtained:

$$\Phi(t) = \frac{\Delta\lambda(t)}{\Delta\lambda_0} = \exp\left[-\left\{\frac{t_{eff}(t)}{\tau_T}\right\}^b\right] \tag{4}$$

In eq 4, $\Delta\lambda(t) = \lambda(t) - \lambda_\infty$, $\Delta\lambda_0 = \lambda_0 - \lambda_\infty$, and $\Delta\lambda(t)/\Delta\lambda_0$ quantifies the normalized distance from equilibrium. In a similar way the PALS data were fitted with an AD-KWW equation, using $\Delta\nu_f(t)/\Delta\nu_{f0}$. The effective time t_{eff} in eq 4 equals

$$\frac{t_{eff}(t)}{t_s} = \frac{(1 + t/t_s)^{1-a} - 1}{1 - a} \tag{5}$$

The effective relaxation time τ_{eff}, introduced by Kovacs,[1] represents the local semilogarithmic slope of the data:

$$\tau_{eff}(t) = -\frac{1}{d \ln \Delta\lambda(t)/dt} \tag{6}$$

The effective relaxation time τ_{eff} is a useful quantity to characterize the aging behavior of a polymer.[34] Values of τ_{eff} are extracted in a straightforward manner, which requires "smoothing" of the experimental data by an appropriate fit function[35] and subsequent differentiation. This procedure is model-independent, i.e., the fit function does not influence the results, and τ_{eff} values thus obtained allow for comparison with data obtained from other techniques, such as volume relaxation experiments.

Experimental Section

Synthesis. TLC analysis was performed on silica gel (Merck, F254). ^{1}H and ^{13}C NMR spectra were measured at 300 MHz (Varian Unity Inova spectrometer) or 400 MHz (Varian VXR 400S spectrometer). ^{1}H chemical shifts are given in ppm (δ) relative to tetramethylsilane (TMS) as internal standard. Reagents, obtained from ACROS and Aldrich, were used as received.

7-(Dimethylamino)quinoline (1). 3-(*N*,*N*-Dimethylamino)aniline dihydrochloride (2.5 g, 12 mmol) was dissolved water (200 mL), and a sodium hydroxide solution (15 mL, 10%) was added. The aqueous solution was extracted with dichloromethane (4 × 50 mL). The combined organic layers were concentrated in vacuo to a brown oil. Then glycerol (4.2 mL), concentrated sulfuric acid (1.6 mL, 96%), and nitrobenzene (3.7 mL) were added. The bulb was fitted with a reflux cooler, and over a period of 1 h the temperature was gradually raised to 100 °C, under a steady stream of nitrogen. The mixture was then stirred at this temperature for 3 h. Finally, the mixture was heated to 140−150 °C for 3 h. After cooling, the reaction mixture was slowly added to an aqueous potassium hydroxide solution (2.5 g in 100 mL) under vigorous stirring. The solution was extracted with dichloromethane (4 × 50 mL). The combined organic layers were dried ($MgSO_4$) and concentrated in vacuo to a black oil, which was purified on silica gel (eluent, chloroform/methanol 99.5/0.5 to chloroform/methanol 95/5) to yield pure **1** (0.53 g, 26%) as a yellow oil.

^{1}H NMR ($CDCl_3$) δ (ppm): 8.73 (1H, d, H2, J = 2.92 Hz), 7.94 (1H, dd, H4, j = 8.13 Hz, j = 1.41 Hz), 7.61 (1H, d, H5, j = 8.65 Hz), 7.12−7.18 (2H, m, H6, H8), 7.07 (1H, dd, H3, j = 8.02, j = 4.27 Hz), 3.07 (6H, s, CH_3N). ^{13}C NMR ($CDCl_3$) δ (ppm): 151.20 (C7), 150.51 (C2), 150.00 (C10), 135.46 (C4), 128.33 (C5), 120.96 (C9), 117.152 (C6), 116.29 (C3), 106.83 (C8), 40.44 (CH_3N).

7-(Dimethylamino)-1-methylquinolinium Tetrafluoroborate (2). To a solution of 7-(dimethylamino)quinoline (**1**) (0.53 g, 3.08 mmol) in 5 mL of methanol, methyl iodide (0.21 mL, 3.39 mmol) was added. The reaction mixture was refluxed overnight. After cooling to room temperature the mixture was diluted with ether. The precipitate was filtered and washed with ether (2 × 50 mL), redissolved in methanol (15 mL), and added to a saturated sodium tetrafluoroborate solution (100 mL). This aqueous solution was then extracted with dichloromethane (4 × 50 mL). The combined organic layers were concentrated in vacuo to a yellow solid, which was purified by recrystallization from methanol/ether to give pure **2** (0.58 g, 69%) as yellow crystals. ^{1}H NMR ($CDCl_3$) δ (ppm): 8.93 (1H, dd, H2, j = 6.04, j = 0.91 Hz), 8.75 (1H, d, H4, j = 7.87 Hz), 8.10 (1H, d, H5, j = 9.34 Hz), 7.58 (1H, dd, H6, j = 9.33 Hz, j = 2.38 Hz), 7.50 (1H, dd, H3, j = 7.88 Hz, j = 6.23 Hz), 6.78 (1H, d, H8, j = 2.01 Hz), 4.32 (3H, s, CH_3N^+), 3.26 (6H, s, $(CH_3)_2N$).

Sample Preparation. The polymers, additive-free polycarbonate and comonomer-free PMMA, were obtained from GE-plastics and Röhm, respectively, and were used as received. Mixtures of polymer with probe (0.05 wt %) were prepared by dissolving **2** (0.001 g) and the polymer (2 g) in freshly distilled dichloromethane (15 mL). Subsequently, the solution was poured onto aluminum foil and left to dry at room temperature (12 h) and under vacuum at 80 °C (3 mmHg, 48 h). PMMA sheets were prepared by hot-pressing at 200

°C, using 0.3 mm aluminum spacers. For PC films hot-pressing at 260 °C, just above the melting temperature, was necessary because PC films cast from solution are semicrystalline.

Fluorescence Spectroscopy. Fluorescence spectra on polymer films were recorded with a Spex/Jobin-Yvon Fluorlog 3 fluorescence spectrometer equipped with a fiber-optic cable in combination with a Linkam hot stage, which was kept under a stream of dry nitrogen during the experiments. The excitation wavelength was 390 nm, and the angle of the incident beam was kept at 45° to the plane of the sample in order to minimize back-reflection of excitation light. Temperature-dependent measurements, for determining λ_{max} vs T plots, were carried out isothermally in steps of 5 K in cooling (from +190 to 50 °C at 10 °C/min for PC and from +160 to 50 °C at 10 °C/min for PMMA). The emission spectra, corrected for the wavelength-dependent sensitivity of the photomultiplier tube, were recorded from 480 to 540 nm. For each temperature 10 spectra were recorded, a procedure that takes ~600 s. Aging experiments were performed after annealing a sample for 15 min at 190 and 160 °C for PC and PMMA, respectively, cooling at 10 °C/min to the aging temperature, and taking spectra at regular time intervals. For each data point one emission spectrum was taken, which requires 150 s. For all experiments it was essential that the spectrometer, the xenon lamp, and the computer were switched on for the entire time of the experiment. Only under these conditions the statistical errors obtained for λ_{max} may be as low as ±0.05 nm. Switching the computer off and on causes an offset in λ_{max} values, which may be on the order of 1 nm.[36] Switching the lamp off between sampling is not an option since restarting the lamp may affect sensitive electronics in the computer. It was proven that the emission monochromator is perfectly stable during long-term experiments and does not exhibit drift.

Data Analysis. From the fluorescence spectra, the intensity I_{max}, the wavelength λ_{max}, and the half-width σ were determined by a least-squares fit that uses 30% of the top of a spectrum. The fit equation of choice is the extreme value function,[37] which has the form

$$I(\lambda) = I_b + I_{max} \exp\{1 - (\lambda - \lambda_{max})/\sigma - \exp[-(\lambda - \lambda_{max})/\sigma]\} \quad (7)$$

where I_b is the "background signal". Using this procedure, values of λ_{max} are obtained in which the statistical error typically is below 0.05 nm. In each series of measurements λ_{max} values were found with larger errors, caused by lamp fluctuations, and these data points were discarded. The least-squares fits of a series of 150 spectra for each aging temperature were performed with MatLab. Values of λ_∞ were estimated by extrapolation of the equilibrium line, i.e., the line of λ vs T above the glass transition temperature, to the actual aging temperature T (Figure 2a,b). The data were therefore approximated using a continuous bilinear least-squares fit. To capture the sharp change in slope at T_g, the abs-function was used:

$$\lambda(T) = \lambda_g + \frac{\alpha_g - \alpha_l}{2}(T - T_g) + \frac{\alpha_l - \alpha_g}{2}|T - T_g| \quad (8)$$

where $\lambda_g = \lambda(T_g)$, α_g is the slope in the glassy state ($T < T_g$), and α_l is that in the liquid or rubbery state ($T > T_g$).

In the nonlinear age-dependent KWW fit $\Delta\lambda(t)$ is normalized to $\Delta\lambda_0$. The value of λ_0 was estimated by a local least-squares fit to $\lambda(t)$, which only covered the first 20 data points of a data set using a simple unmodified KWW function.[38]

$$\lambda(t) = \lambda_0 e^{-at^b} \quad (9)$$

Unavoidable scatter in our data makes a direct fit with the age-dependent KWW cumbersome as false minima are often encountered in the least-squares fits. A convenient solution to this problem is the application of a polynomial in ln(t):

$$\ln\left(\frac{\Delta\lambda(t)}{\Delta\lambda_0}\right) = \sum_{k=0}^{n=4} a_k \ln^k t \quad (10)$$

Scheme 1. Synthesis of 2 Using a Skraup Procedure

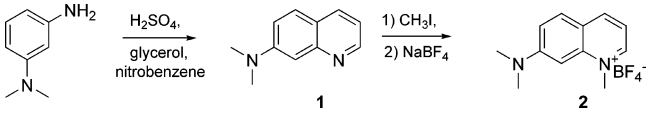

The ln(t) sum has the advantage of being a linear least-squares fit. Fitting the experimental data with eq 10 generated a "smoothed" data set that could be used as input for an age-dependent KWW fit. Rewriting the age-dependent KWW function, eq 4, results in eq 11, which was simplified to eq 12.

$$\ln\left(\frac{\Delta\lambda(t)}{\Delta\lambda_0}\right) = -\left(\frac{t_s}{(1-a)\tau_T}\right)^b \left[\left(1 + \frac{t}{t_s}\right)^{1-a} - 1\right]^b \quad (11)$$

$$\ln\left(\frac{\Delta\lambda(t)}{\Delta\lambda_0}\right) = -a'[(1 + b't)^{c'} - 1]^{d'} \quad (12)$$

Here $a' = (1/b'c'\tau_T)^{d'}$, $b' = 1/t_s$, $c' = 1 - a$, and $d' = b$.

Results

Synthesis. The synthesis of 7-(dimethylamino)quinoline (**1**), according to Scheme 1, was first described by Bradford et al.[39] using the Skraup reaction for making the quinoline structure. Along with the desired 7-(dimethylamino)-isomer, a small amount of the 5-isomer is formed, which is difficult to remove. More traditional Skraup conditions,[40] using 98% sulfuric acid and nitrobenzene as the oxidant, gave a product free of the 5-(dimethylamino)-isomer. A major disadvantage of this procedure is the severe reaction conditions, which result in the production of large amounts of tar and yields that may be as low as 5%. However, careful heating under a nitrogen atmosphere enabled us to obtain a yield of 26%. Both the starting material and product of this reaction are sensitive to air oxidation, in their nonprotonated form. Alkylation of **1** with methyl iodide and subsequent ion exchange, using sodium tetrafluoroborate, gave 7-(dimethylamino)-1-methylquinolinium tetrafluoroborate (**2**) in good yield.

Employing the synthetic procedure described above, various alkyl chains may be attached to the amino functionality, while functionalized moieties may be attached at the quinolinium nitrogen. In all cases, however, the Skraup procedure is severely limiting the practical use of this synthesis. Further details concerning this reaction and alternative procedures to synthesize **2** and its derivatives will be presented elsewhere.

Fluorescence Spectroscopy. Recent research has shown that charge transfer and charge resonance probes, notably nitrostilbenes and stilbazolium salts, are excellent probes for the monitoring of polymerization reactions[25,41] and characterizing polymers.[26−29] However, the relatively small changes in medium mobility associated with physical aging along with harsh processing and measuring conditions impose severe constraints on the probes in terms of photochemical and thermal stability. Neither stilbazolium salts nor (dialkylamino)nitrostilbene probes were stable enough to withstand these conditions, which include annealing at temperatures up to 260 °C and light exposure at elevated temperatures over long periods of time. Thermal bleaching, photochemical degradation, and cis−trans isomerizations were observed for these probes.[42]

To eliminate degradation and (photo)isomerization reactions, fluorescent probes containing a rigid fully aromatic chromophore are required. On the basis of these considerations, we decided to synthesize **2**, one of the simplest and smallest charge resonance probes that possess a rigid π-system connecting the donor and the acceptor. Table 1 shows the absorption and

Table 1. Spectroscopic Properties of 2 in Different Solvents

solvent	λ_{max}(abs) (nm)	λ_{max}(em) (nm)	Stokes shift (nm)
ethyl acetate	433	537	104
tetrahydrofuran	435	530	95
dichloromethane	442	506	64

emission properties of **2** in different solvents. A Stokes shift of up to 104 nm in ethyl acetate is observed, which is remarkably high for such a small quinolinium chromophore. The photochemical stability of **2** in a polymer matrix was established by exposing a sample of doped PMMA, which had aged for 14 days at room temperature, to 40 sequential measurements with the highest possible intensity of excitation light (~50 W/m^2 at 390 nm). This gave no decrease in intensity, nor was there any change in the shape and position of the emission spectra. Annealing of PC samples containing **2** at a temperature of 260 °C did not result in loss of emission or the noticeable presence of bleaching products and demonstrated the remarkable thermal stability of the probe.

A typical emission spectrum of **2** in a polycarbonate matrix, in which the data points were fitted using the extreme value function, is shown in Figure 1. The least-squares fit of the top of the emission spectrum allowed us to determine the position of the emission maximum with a typical error of 0.03−0.05 nm in each series of experiments. Since the shape of the emission spectra does not change during aging, we could use one fit function. In this way, reliable and accurate values for the emission wavelength of **2** during aging experiments were obtained.

Determination of T_g by Temperature-Dependent Emission. A prerequisite for probes capable of monitoring physical aging by changes in emission wavelength λ_{max}, apart from long-term stability, is the ability to detect the glass transition temperature, T_g.[16,43] Emission wavelengths, obtained during cooling, are plotted as a function of temperature in parts a and b of Figure 2 for PC and PMMA, respectively. Figure 2a shows that the emission wavelength of **2** in PC is a linear function of temperature, both below and above the glass transition temperature. A distinct change in slope is observed at the glass transition temperature, and below T_g an excess emission wavelength $\Delta\lambda$ is defined by the difference between the experimental emission wavelength and the emission wavelength on the extrapolated equilibrium line.[44]

In Figure 2b, the emission wavelength of **2** doped in PMMA is plotted as a function of temperature. The change in gradient upon passage of T_g is slightly stronger for PMMA compared to PC. Also, the emission of **2** in PMMA is ~20 nm blue shifted compared to the emission from **2** in PC, and this may be attributed to the fact that PMMA is a less polarizable medium.

The straight lines in Figure 2a,b suggest to a linear relationship between the specific volume v_s of the host polymer and

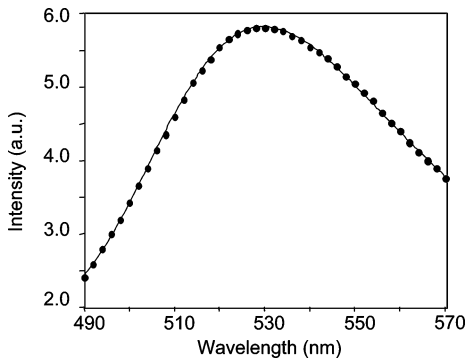

Figure 1. Emission spectrum of **2** in PC (λ_{max} = 529.9 nm at 25 °C).

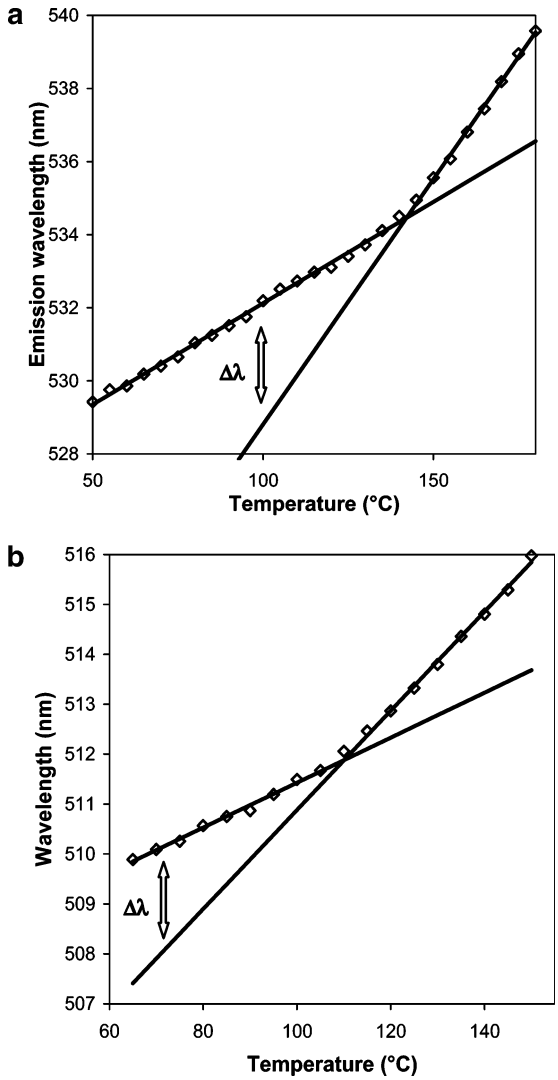

Figure 2. Emission wavelength of **2** taken as a function of the temperature in PC (a) and in PMMA (b).

λ_{max}. This assumption is confirmed by Figure 3 in which v_s, taken from ref 2a, is plotted against λ_{max} of **2** in both for PC and PMMA. The linear relationship, which is valid from low temperatures up to temperatures well above T_g, corroborates that the changes in λ_{max} during aging are proportional to those in v_s. This implies that, like in volume relaxation experiments, the distance from equilibrium is known throughout the aging process. A qualitative explanation for the relationship between λ_{max} and v_s will be given in the discussion.

Physical Aging Measurements. Figure 4 shows the emission wavelength λ_{max} of **2** as a function of the time for an aging experiment in PC performed at 65 °C. Along with the experimental data, which have a statistical error of 0.03 nm, the age-dependent KWW fit is shown. Since the excess emission wavelength $\Delta\lambda$ at 65 °C is 6.1 nm, the 0.03 nm scatter allows for accurate measurements. Similar plots are obtained at the other temperatures. In Figure 5, $\ln[\Delta\lambda(t)/\Delta\lambda_0]$ is plotted as a function of $\log(t)$ for all aging experiments, along with the corresponding age-dependent KWW fits. The extent of relaxation, i.e., the fraction of $\Delta\lambda$ lost at the end of the experiment, is limited to 28, 12, 5, and 3% at 128, 100, 65, and 25 °C, respectively. Figure 5 clearly shows that aging proceeds much faster at higher temperatures because the system is more mobile at elevated temperatures.[45]

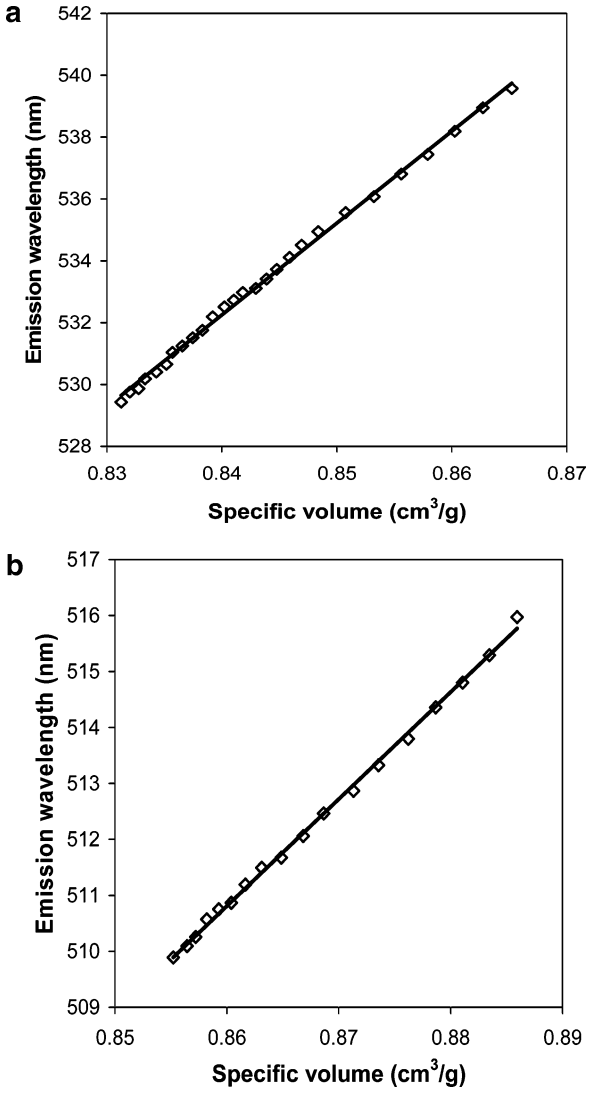

Figure 3. Specific volume ν_s taken from ref 2a, plotted against the emission maximum λ_{max} of **2** in PC (a) and PMMA (b).

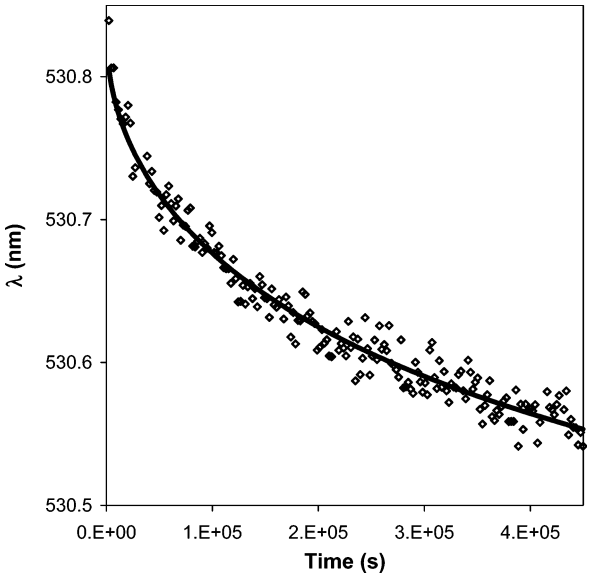

Figure 4. Emission wavelength of **2** as a function of time in PC at 65 °C along with the age-dependent KWW fit.

In Figure 6, the effective relaxation time τ_{eff}, derived from the age-dependent KWW fits, is plotted versus the relaxation time on a double-logarithmic scale. For each aging temperature

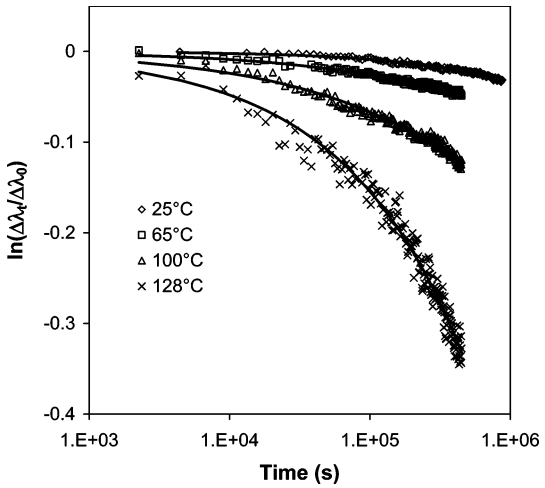

Figure 5. Relaxation data of PC obtained at different temperatures by fluorescence along with the age-dependent KWW fits.

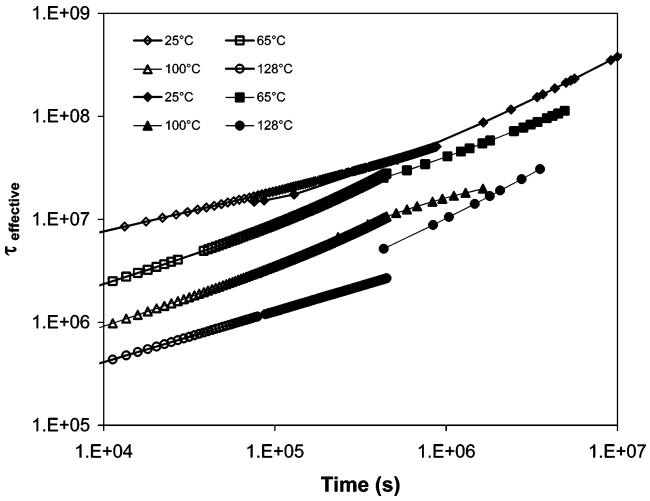

Figure 6. Effective relaxation times τ_{eff} of PC derived from age-dependent KWW fits on the data obtained by fluorescence (open symbols) and PALS (filled symbols). The PALS data were taken from ref 30.

Table 2. Age-Dependent KWW Parameters for PC Obtained by Fluorescence

T (°C)	25	65	100	128
$T - T_g$	115	75	40	12
τ_T (s)	2.1×10^8	1.7×10^8	3.4×10^7	2.0×10^6
b	0.62	0.48	0.46	0.60
t_s (s)	3.0×10^6	4.2×10^5	5.6×10^5	3.3×10^5
a	0.95	0.98	0.95	0.80
$\Delta\lambda_0$	9.22	6.07	3.31	1.11
extent of relaxation (%)	3.1	4.5	12	25

the effective relaxation time τ_{eff} increases with time, an observation that is characteristic for a self-retarding process. In Figure 6, we have also plotted the effective relaxation times taken from the PALS experiments in ref 30, and it is evident that τ_{eff} values determined by fluorescence and PALS are in quite good agreement, except for the data taken at 128 °C. It should be noted that fluorescence data, taken over a relatively short time interval, and the PALS data provide complementary information. Finally, it is worth mentioning that the effective relaxation times τ_{eff}, recorded at 25 °C by PALS and fluorescence, are similar to those measured by dilatometry.[46]

Table 2 summarizes the data obtained from the age-dependent KWW fits. The temperature-dependent relaxation time τ_T, i.e., the relaxation time at $t = 0$, decreases 2 orders of magnitude as the aging temperature increases. The values for the KWW

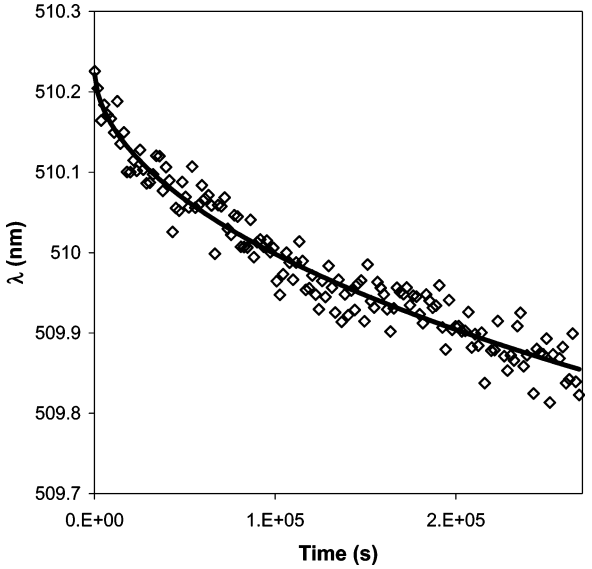

Figure 7. Emission wavelength of **2** as a function of time in PMMA at 70 °C along with the age-dependent KWW fit.

stretching parameter *b* range from 0.5 to 0.6 and shows that the physical aging proceeds with a distribution in relaxation times. It should be noted that the values for τ_T and *b* are in good agreement with those that are determined by KWW fits over the first 20 data points at each temperature. The other parameters in Table 2 are the scaling time t_s and the aging power *a*. For the aging power *a* values close to 1 are observed, and this indicates "logarithmic" aging in PC, i.e., aging with a high degree of self-retardation. Values of the scaling time t_s decrease with increasing temperature, and this implies that at higher temperature the age-dependent relaxation time τ_a increases faster in time. Finally, it should be noted that although the fits obtained with the AD-KWW functions are very satisfactory, the errors in the individual parameters are substantial. In particular, the values found for the scaling time t_s and the aging power *a*, which describe the age-dependent relaxation time τ_a, are error-prone and should be interpreted with care.

Figure 7 shows the decay in the emission wavelength λ_{max} as a function of time for an aging experiment performed in PMMA at 70 °C, along with the age-dependent KWW fit. The statistical error in this data set is 0.05, significantly larger than in the PC experiments. Similar decay curves are obtained at the other aging temperatures. Figure 8 plots the normalized distance from equilibrium $\Delta\lambda(t)/\Delta\lambda_0$ as a function of the aging time *t* at different aging temperatures, and faster relaxations are observed at higher temperatures. It should be noted that the extent of relaxation in PMMA is substantially higher than in PC; 83, 25, and 18% for the experiments performed at 100, 85, and 70 °C, respectively, and this reflects the faster aging kinetics in PMMA, which is partly due to its lower glass transition temperature. Finally, it should be noted that the τ_{eff} values found at 70 and 85 °C correspond well with those obtained from volume relaxation described in ref 47.

Table 3 shows the fitting parameters for all temperatures obtained with age-dependent KWW fits. The temperature-dependent relaxation time τ_T decreases as the aging temperature increases. Substantially lower values are obtained than in PC, indicating a faster aging process. Like in PC, values for the KWW stretching parameter *b* around 0.5 are found. Once more, the values of τ_T and *b* from the AD-KWW fits correspond well to those determined by KWW fits over the first 20 data points. For the aging power *a*, values around 0.5 are found. The scaling

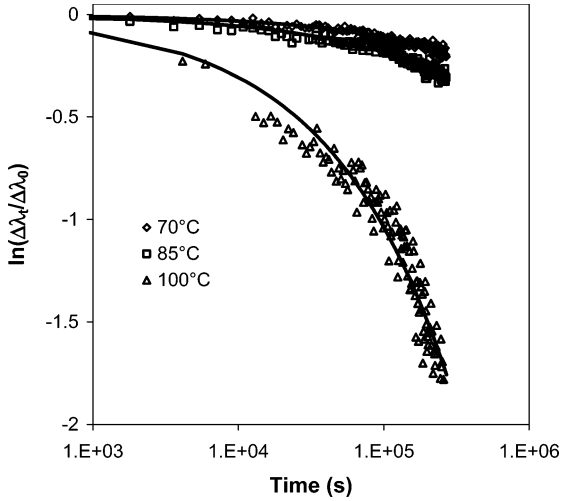

Figure 8. Relaxation data of PMMA obtained at different temperatures by fluorescence along with the age-dependent KWW fits.

Table 3. Age-Dependent KWW Parameters for PMMA Obtained by Fluorescence

T (°C)	70	85	100
$T - T_g$	38	23	8
τ_T (s)	5.9×10^6	2.7×10^6	8.4×10^4
b	0.54	0.51	0.50
t_s (s)	6.0×10^6	4.6×10^6	1.6×10^5
a	0.60	0.47	0.42
$\Delta\lambda_0$	2.16	1.38	0.59
extent of relaxation (%)	17	26	87

times t_s decrease with increasing temperature and have relatively large values. Both the low values of *a* and the relatively large values of t_s indicate a relatively slow increase of τ_a in time, which indicates that the aging process in PMMA proceeds with a lower degree of self-retardation than the aging of PC.

Discussion

We have demonstrated a new method for investigating physical aging by fluorescence spectroscopy. From the blue shift in fluorescence of the color-shifting mobility-sensitive probe **2**, the aging process in PC and PMMA was measured in a straightforward manner. Using **2**, effective relaxation times τ_{eff} of both PC and PMMA were obtained over a range of temperatures and aging times. In addition, the relaxation process was described by an age-dependent KWW equation. The effective relaxation times of PC derived from the fluorescence of **2** corresponded well with those obtained by PALS measurements, with the exception of those obtained by the high-temperature experiment taken at 128 °C. In addition, values of τ_{eff} obtained by volume relaxation obtained at 23 °C,[46] and our fluorescence experiments at 25 °C are similar. For PMMA, faster physical aging was observed because this polymer was investigated at temperatures closer to its T_g and because the aging of PMMA is less self-retarding. Unfortunately, we have no PALS data for PMMA, but the effective relaxation times obtained by fluorescence correspond well to those extracted from volume relaxation experiments,[47] except for those obtained by the high-temperature experiment taken at 100 °C. These results confirm that physical aging can be determined reliably from the fluorescence of **2**. Only at high temperatures, the reliability of the results obtained by fluorescence is no longer warranted. This may be explained by the following arguments. First of all, the fluorescence quantum yield goes down with increasing temperature, and therefore, the accuracy of the λ_{max} determination decreases. Furthermore, the total blue shift during aging ($\Delta\lambda$ in

Figure 2) decreases, and this leads to a further increase in the signal-to-noise ratio. Finally, probe degradation becomes more likely at higher temperatures. Although we have no indication of substantial probe degradation at high-temperature aging experiments, the low τ_{eff} values measured at longer aging times would be consistent with bleaching. This is so because probe bleaching would result in a decreased self-absorption and an apparent blue shift in emission. Although probe bleaching cannot be prevented, lowering the extent of self-absorption by lowering the probe concentration would decrease its effect on the measured λ_{max} values.

A prerequisite for probes capable of monitoring physical aging, apart from long-term stability, is the ability to detect the glass transition temperature T_g. Our probe is capable of detecting T_g because the emission wavelength of the probe scales with the specific volume of the host polymer. This relationship was proven for PMMA and PC by comparing temperature-dependent emission of **2** with specific volume data taken from the literature.[2a] This relationship also connects the emission wavelength of **2** with the free volume v_f, determined by PALS, and allows for direct comparison with volume relaxation experiments.

Although the exact mechanism by which the polymer stabilizes the probe is still under investigation, a qualitative explanation of the probe behavior is easily constructed. The observed blue shifts in the probe's emission are rationalized by assuming charge transfer in the probe's excited state and stabilization of the strongly dipolar excited state, during its lifetime of ~10−15 ns,[48] by dipole−dipole interactions. Furthermore, it is obvious that a decrease in specific or rather free volume during an aging experiment induces a decreased mobility of the polar groups in the polymer. Therefore, this decreased medium mobility results in a weaker stabilization of the probe's excited state, resulting in a higher energy emission. This is consistent with the experimentally obtained blue shifts in emission.

Using color-shifting fluorescent probes for studying physical aging has distinct advantages. These are the inherent advantages of using fluorescent probes already mentioned in the Introduction, but on top of that, using color-shifting probes instead of the more conventional intensity changing ones does significantly broaden the scope of the methodology. Color-shifting probes are self-referencing, and therefore many requirements concerning sample composition, sample geometry, sample positioning, and equipment stability no longer apply.[49] The only stringent requirement for employing wavelength-shifting probes is a limited and stable degree of (self) absorption by the probe or by other species. Apart from obtaining spatial resolution in an uncomplicated fashion, the study of physical aging in nonhomogeneous polymeric materials is an attractive proposition for the use of this type of fluorescent probes. In this context it is worth mentioning that we have already measured glass transition temperatures in semicrystalline polymers and in polymer blends.[22] In view of the growing interest in the effects of confinement on relaxation phenomena, it should be noted that color-shifting probes can be employed for measuring aging in confined systems other than ultrathin films, i.e., two- and three-dimensional confinement. Another point worth mentioning is that since the emission wavelength is a state variable, the distance from equilibrium in complex systems is known throughout the aging experiment, with spatial resolution. This offers opportunities to investigating the relaxation dynamics in real-life polymeric objects, for example the influence of mechanical stress on physical aging, in great detail.

Finally, we wish to emphasize that by the experiments presented in this paper we have proven the concept of using a color-shifting mobility-sensitive probe for measuring physical aging. To fully exploit this methodology, and to investigate physical aging itself, however, additional research is required. For this research, we strongly recommend adaptation of the instrumentation we have used so far because the speed and reliability of the measurements are limited basically by the spectrometer and not by the probe. Our first adaptation is the use of a blue laser as an external light source, since this would allow for longer aging experiments. Using a laser would also provide internal calibration of the spectra and allow for spatial resolution by changing the position of the excitation beam. Detection of the probe emission by a CCD detector, instead of a monochromator equipped with a photomultiplier tube, would bring down acquisition times to the subsecond level,[50] so that the early stages of the physical aging process can be monitored. In addition, this adaptation might improve the long-term stability of the setup since a CCD detector does not contain moving parts.

Conclusions

We have demonstrated that, by recording the blue shift in the emission of the color-shifting mobility sensitive fluorescent probe **2**, the physical aging process of the host polymers in which the probe was dissolved was measured. This unique methodology relies on the fact that the emission wavelength of **2** scales with the specific volume of the polymer. Effective relaxation times τ_{eff} obtained from the fluorescence of **2** in PC samples are comparable with those recently obtained by PALS and volume relaxation measurements. Similar effective relaxation times were also obtained by fluorescence and by volume relaxation experiments in PMMA. These observations prove the reliability of the fluorescent probe technique. Another key issue is the stability of **2**. Photochemical degradation was not observed, and no signs of probe degradation were noticed during aging experiments. This outstanding stability is crucial for the successful application of color-shifting fluorescent probes for investigating physical aging.

We have demonstrated that the fluorescent probe method is convenient and fast[49] and works well at a broad range of temperatures. For measurements at the "lower" temperature range, accurate results are obtained. Only for measurements at high temperatures, close to T_g, relaxation times have not been determined accurately. The most promising application of the color-shifting fluorescent probe methodology is for measuring physical aging in opaque, scattering, and inhomogeneous samples. The effects of confinement in such complex systems should also be accessible by this technique. Further research, employing color-shifting fluorescent probes for investigating the relaxation dynamics in complex media, which are virtually inaccessible by other experimental techniques, is currently undertaken.

Acknowledgment. The authors thank the reviewers for their helpful comments and suggestions. The Dutch Polymer Institute is gratefully acknowledged for support of this investigation under Project nr. #151.

Supporting Information Available: Figures showing DSC cooling curves for PC and PMMA doped with 0.05% **2**. This material is available free of charge via the Internet at http://pubs.acs.org.

References and Notes

(1) Kovacs, A. J. *Adv. Polym. Sci.* **1963**, *3*, 394.

(2) (a) Greiner, R.; Schwarzl, F. R. *Rheol. Acta* **1984**, *23*, 378. (b) Greiner, R.; Schwarzl, F. R. *Colloid Polym. Sci.* **1989**, *267*, 39.
(3) (a) Brunacci, A.; Cowie, J. M. G.; Ferguson, R.; McEwen, I. J. *Polymer* **1997**, *38*, 865. (b) Brunacci, A.; Cowie, J. M. G.; Ferguson, R.; McEwen, I. J. *Polymer* **1997**, *38*, 3263.
(4) Hourston, D. J.; Song, M.; Hammiche, A.; Pollock, H. M.; Reading, M. *Polymer* **1996**, *37*, 243.
(5) Struik, L. C. E. In *Physical Aging in Amorphous Polymers and Other Materials*; Elsevier: Amsterdam, 1978.
(6) Hutchinson, J. M. *Prog. Polym. Sci.* **1995**, *20*, 703.
(7) (a) McKenna, G. B. In *Glass Formation and Glassy Behavior in Comprehensive Polymer Science*; Allen, G., et al., Eds.; Pergamon Press: Oxford, 1989; Vol. 2, Chapter 10, pp 169−189. (b) Angell, C. A.; Ngai, K. L.; McKenna, G. B.; McMillan, P. F.; Martin, S. W. *J. Appl. Phys.* **2000**, *88*, 3113.
(8) Hodge, I. M. *J. Non-Cryst. Solids* **1994**, *169*, 211.
(9) Alvarez, C.; Correia, N. T.; Ramos, J. J. M.; Fernandes, A. C. *Polymer* **2000**, *41*, 2907.
(10) Echeverria, I.; Kolek, P. L.; Plazek, D. J. *J. Non-Cryst. Solids* **2003**, *324*, 242.
(11) Pethrick, R. A.; Davis, W. J. *Polym. Int.* **1998**, *47*, 65.
(12) Fulcher, G. S. *J. Am. Ceram. Soc.* **1925**, *8*, 339.
(13) Vogel, H. *Z. Phys.* **1921**, *22*, 645.
(14) Tammann, G.; Hesse, G. Z. *Anorg. Allg. Chem.* **1926**, *156*, 245.
(15) O'Connell, P. A.; McKenna, G. B. *J. Chem. Phys.* **1999**, *110*, 11054.
(16) Loutfy, R. O. *Macromolecules* **1980**, *14*, 270.
(17) (a) Royal, J. S.; Torkelson, J. M. *Macromolecules* **1993**, *26*, 5331. (b) Royal, J. S.; Torkelson, J. M. *Macromolecules* **1990**, *23*, 3536.
(18) Royal, J. S.; Torkelson, J. M. *Macromolecules* **1992**, *25*, 1705.
(19) Kovacs, A. J.; Aklonis, J. J.; Hutchinson, J. M.; Ramos, A. R. *J. Polym. Sci., Part B* **1979**, *17*, 1097.
(20) (a) Priestley, R. D.; Broadbelt, L. J.; Torkelson, J. M. *Macromolecules* **2005**, *38*, 654. (b) Priestley, R. D.; Ellison, C. J.; Broadbelt, L. J.; Torkelson, J. M. *Science* **2005**, *309*, 456.
(21) For aging experiments with other probes see: (a) Guo, R. K.; Tazuke, S. *Macromolecules* **1989**, *22*, 3266. (b) Meyer, E. F.; Jamieson, A. M.; Simha, R.; Palmen, J. H. M.; Booij, H. C.; Maurer, F. H. J. *Polymer* **1990**, *31*, 243.
(22) From the emission of **2** dissolved in semicrystalline polymers and polymer blends, the glass transition temperature of the polymer has been determined accurately in a straightforward manner. See: Jager, W. F.; van den Berg, O.; Picken, S. J., accepted for *Macromol. Symp.*
(23) Paczkowski, J.; Neckers, D. C. *Macromolecules* **1992**, *25*, 548.
(24) van Ramensdonk, H. J.; Vos, M.; Verhoeven, J. W.; Möhlmann, G. R.; Tissink, N. A.; Meesen, A. W. *Polymer* **1987**, 951.
(25) Jager, W. F.; Kudasheva, D.; Neckers, D. C. *Macromolecules* **1996**, *29*, 7351.
(26) Shea, K. J.; Sasaki, D. Y.; Stoddard, G. J. *Macromolecules* **1989**, *22*, 1721.
(27) Ellison, C. J.; Miller, K. E.; Torkelson, J. M. *Polymer* **2004**, *45*, 2623.
(28) Hofstraat, J. W.; Veurink, J.; Gebben, B.; Verheij, H. J.; Verhoeven, J. W. *J. Fluoresc.* **1998**, *8*, 335. (b) Verheij, H. J.; Gebben, B.; Hofstraat, J. W.; Verhoeven, J. W. *J. Polym. Sci., Part A* **1995**, *33*, 399.
(29) van den Berg, O.; Sengers, W. G. F.; Jager, W. F.; Picken, S. J.; Wübbenhorst, M. *Macromolecules* **2004**, *37*, 2460.
(30) Cangialosi, D.; Wübbenhorst, M.; Schut, H.; Veen, A. V.; Picken, S. J. *Phys. Rev. B* **2004**, *69*, 134206.
(31) Goldbach, G.; Rehage, G. *Rheol. Acta* **1967**, *6*, 30.
(32) van Turnhout, J.; Wübbenhorst, M. *J. Non-Cryst. Solids* **2002**, *305*, 50.
(33) Note that in our probe experiments the aging time *coincides* with the running time. This differs basically from most other aging experiments, e.g., creep measurements, where the sample is *first preaged* during an elapsed time t_e after which the shear stress is applied; the total aging time then equals $t + t_e$.
(34) Note that if $b = 1$, i.e., for "Debye aging" with a single relaxation time, $\tau_{eff}(t)$ equals $\tau(T,t)$.
(35) The appropriate fit function can be either the age-dependent KWW function (eq 4) or a polynomial in $\ln(t)$ (eq 10). The values of τ_{eff} obtained by either using eq 4 or eq 10 are virtually identical.
(36) It should be stated explicitly that the ±1 nm offset that is observed in λ_{max} values upon restarting the spectrometer is caused by the complex and unstable software and is not a hardware problem.
(37) Other peak functions, such as those for a Lorentz or Gauss peak, were also tried, but they had to be disqualified as none of them account for the skewness observed in the emission spectra of **2**-doped polymers.
(38) The λ_0 value derived from the $\lambda-T$ data could not be used as a starting value because this value may show an offset in the order of ±1 nm due to recalibration of the spectrometer.
(39) Bradford, L.; Elliott, T. J.; Rowe, F. M. *J. Chem. Soc.* **1947**, 437.
(40) Mosettig, E.; Robinson, R. A. *J. Am. Chem. Soc.* **1935**, *57*, 7.
(41) (a) Jager, W. F.; Norder, B. *Macromolecules* **2000**, *33*, 8576. (b) Jager, W. F.; van den Berg, O. In *Photoinitiated Polymerization*; ACS Symposium Series 847; Belfield, K. D., Crivello, J. V., Eds.; American Chemical Society: Washington, DC, 2003; Vol. 847, p 426.
(42) In this perspective, it should be noted that for a number of related dyes the cis−trans isomerization has been exploited to track changes in free volume distributions in several polymers. See: Victor, J. G.; Torkelson, J. M. *Macromolecules* **1988**, *21*, 3490.
(43) (a) Ellison, C. J.; Torkelson, J. M. *Nat. Mater.* **2003**, *2*, 695. (b) Ellison, C. J.; Kim, S. D.; Hall, D. B.; Torkelson, J. M. *Eur. Phys. J. E* **2002**, *8*, 155−166.
(44) In a similar manner, excess specific volume is obtained in volume relaxation experiments.
(45) This might be confusing in view of *absolute* rates of physical aging reported by others. However, in our modeling of the kinetics of physical aging, i.e., eq 4, the emission wavelengths are normalized to the distance from equilibrium.
(46) Wimberger-Friedl, R.; de Bruin, J. G. *Macromolecules* **1996**, *29*, 4992.
(47) Slobodian, P.; Říha, P.; Lengálová, A.; Hadač, J.; Sáha, P.; Kubát, J. *J. Non-Cryst. Solids* **2004**, *344*, 148.
(48) Jager, W. F.; van den Berg, O.; Donker, H.; Picken, S. J. *Polym. Mater. Sci. Eng.* **2004**, *90*, 570.
(49) Employing intensity changing probes requires stable equipment, on both the excitation and emission side, producing reproducible spectra over long periods of time. Dimensionally stable clear and nonscattering samples are required, especially when spatial resolution is desired.
(50) Replacing our conventional spectrometer by a CCD-based device would enable fast data acquisition (see ref 40b).

MA048329I